

On the Extreme Ultraviolet Emission from Galaxy Clusters

John S. Arabadjis and Joel N. Bregman
 Dept. of Astronomy, University of Michigan
 Ann Arbor, MI 48109-1090
 jsa@astro.lsa.umich.edu, jbregman@umich.edu

ABSTRACT

An extremely soft X-ray excess throughout galaxy clusters has been claimed as a new feature of these systems, with important physical implications. We have reexamined this feature in the five clusters for which it has been discussed, using the most recent X-ray absorption cross sections, X-ray data processing techniques, and a consistent set of HI data. For the Virgo cluster, we find that the spectrum can be fit with a single-temperature thermal plasma and with an X-ray absorption column that is not significantly different than the Galactic HI column. The result for Abell 1367, Abell 1656 (Coma), Abell 1795, and Abell 2199 is similar in that the difference between the X-ray absorption column and the Galactic HI column is less than 3σ for $\text{He}/\text{H} = 0.09$, and for $\text{He}/\text{H} = 0.10$ only one cluster location leads to a Galactic HI column more than 3σ above the X-ray absorption column (Coma, with one location with a 3.6σ difference). We conclude that there is no strong evidence for the extremely soft X-ray excess in galaxy clusters.

1. Introduction

One of the surprises in the studies of galaxy clusters is that they were detected by the *EUVE* (Lieu *et al.* 1996c), an instrument whose primarily goals were the studies of stars and gas in the local neighborhood. The *EUVE* has both imaging and spectroscopic capabilities that operate in the spectral range 70-760 Å (177-16.3 eV; Haisch, Bowyer, and Malina 1993). For high latitude sight lines of low Galactic N_{HI} ($1.0 \times 10^{20} \text{ cm}^{-2}$), the optical depth $\tau = 2.8$ at 130 eV and $\tau = 1.16$ at 180 eV, so 6-30% of the emission will be unabsorbed, permitting the detection of bright soft X-ray sources. Soft X-ray emission also can be detected with the *ROSAT* PSPC, which has an energy response extending below 150 eV and has significantly more collecting area than the *EUVE* at energies of significant transmission of X-rays. At 0.13 keV (the peak sensitivity of the *EUVE* Lexan/boron detector) the effective area is 28 cm^2 , compared with 40 cm^2 for the *ROSAT* PSPC. At

0.155 keV, the *EUVE* effective area has dropped to less than cm^2 , whereas for the PSPC it is greater than 100 cm^2 .

In their study of the Virgo cluster, centered on M87, Lieu *et al.* (1996b) were unable to successfully fit the data with a single-temperature spectral model at the ambient cluster temperature (about 2 keV) and with the X-ray absorbing column fixed at the Galactic N_{HI} . The failure to fit the data was due to a large excess of soft residuals, indicating that there was an additional soft component. A two-temperature model led to an acceptable fit when the soft component had a temperature of about 0.05 keV, implying that large amounts of gas at $5 \times 10^5 \text{ K}$ are present. An exciting consequence of this observation is that the cooling rate of the gas, if in a steady-state, would be at least $340 \text{ M}_\odot \text{ y}^{-1}$, at least a factor of 30 greater than the value determined from the standard cooling flow picture of $10 \text{ M}_\odot \text{ y}^{-1}$ (Fabian, Nulsen, and Canizares 1984).

The presence of such a large amount of cooling gas has a variety of consequences, such as the a mass of low temperature component that was comparable to the virial mass of the cluster (Fabian 1996; Sarazin and Lieu 1998). Also, there were observable consequences, such as emission from the O VI species, which was not detected in the same clusters in which the soft component was present (Dixon, Hurwitz, and Ferguson 1996). Faced with these difficulties, another suggestion was proposed for this emission: the soft X-ray component was due to inverse Compton radiation of the cosmic microwave background by low energy cosmic ray electrons (Sarazin and Lieu 1998).

Since the original study of the Virgo cluster, several other clusters have been studied by the same group: Abell 1656 (Coma), Abell 1795, Abell 2199, and Abell 1367 (Lieu *et al.* 1996a,b,c; Mittaz, Lieu, and Lockman 1998; Table 1). In each case, the excess X-ray emission is detected at approximately the same energy, about 0.15-0.25 keV. One might expect a thermal feature to occur at the same energy in different clusters, but it seems surprising to us that a nonthermal component would always appear at the same energy.

Here we take a different approach to examining the phenomenon of the excess soft emission. Since the soft emission becomes less prominent, and may disappear if lower Galactic absorption columns were possible, we ask whether it is feasible to achieve a spectral fit without the soft component and for absorption columns consistent with the Galactic N_{HI} . Although we do not disagree with the fitting method employed by Lieu and collaborators, there has recently been a downward revision of the X-ray cross section at these energies, due to improved cross sections for He I. We examine whether this change to the X-ray cross section permits an acceptable spectral fit without a soft component.

2. Data Processing and Analysis

One of the central issues in the measurement of the soft component in galaxy clusters is the correction for the absorption of X-rays by Galactic gas. A very important issue for this absorption, which has only been rectified recently, is the value for the cross section of He (Fig. reff1). At energies in the 150-250 eV range, where most of the absorption occurs, He accounts for about 71% of the cross section, with hydrogen providing the remainder. The commonly used cross section of Bałucińska-Church and McCammon (1993) adopted a cross section for He that is based upon data from Marr and West (1976). These are 18-19% larger than the recent determination of Yan, Sadeghpour, and Dalgarno (1998), which is similar to the determinations of Samson *et al.* (1994), Bizeau and Wuilleumier (1995), and Morrison and McCammon (1983, which is in turn based upon data from Henke *et al.* 1982). By using the improved cross section for He, the total cross section at 150 eV decreases by 13%, thus causing a rise in the expected soft continuum in a single temperature fit (for fixed N_{HI}).

Using the new absorption cross sections, we have addressed the issue of whether the X-ray spectra from the clusters showing soft component can be fit without employing a soft component. In this case, we let the value for the Galactic absorption column be a parameter that is fit, rather than fixing it. If a successful fit is discovered, as determined from an acceptable χ^2 , we examine whether the fit value for the Galactic absorption column is consistent or inconsistent with the Galactic N_{HI} value.

The X-ray spectral fitting is performed on our data as discussed by Arabadjis and Bregman (1998), whereby the *ROSAT* PSPC data are corrected for gain fluctuations across the image plane (through PCPICOR) and periods of time with high backgrounds are removed, which removes only a few percent of the data at most. Two concentric adjacent annuli, with point sources removed, were used to produce a pair of spectrally well-behaved X-ray sources for each cluster (Table 2). (In A2199 and A1795 the annuli are chosen specifically to avoid the known cooling flow regions.) The exception to this is Coma (Abell 1656), where we sought to avoid the galaxies near the center of the cluster. In that case we chose two circular regions with radii of 3' near the center but avoiding the member galaxies. Background spectra were generally taken from annuli with widths between 2-4' and radii between 15 and 20', again with point sources removed.

The temperatures and redshift of each cluster were taken from White, Jones and Forman (1997), and the metallicity assumed for each cluster was 0.3. It should be noted that other recent temperature determinations (e.g. White *et al.* 1994; Donnelly *et al.* 1998) are within a few tenths of a keV of our adopted values, the effect of which is minimal upon the derived columns. This leaves two free parameters in each fit, the intervening column and

the spectral normalization. The exception to this is Virgo, where we fit for the temperature along with the column and normalization, and set the abundance to 0.34 (Hwang *et al.* 1997). The resulting temperatures, 1.60 ± 0.06 and 1.67 ± 0.11 keV, are consistent with the temperature profiles derived for Virgo by Nulsen and Böhringer (1995) and D’Acri, De Grandi, and Molendi (1998). The derived columns are not particularly sensitive to changes of the order of $\delta T \sim 0.2$ K and $\delta z \sim 0.2$, changing by less than 5%.

Spectral fitting is performed using XSPEC version 10 (see, e.g., Arnaud 1996), with the important change that we have put in the new cross sections for He I of Yan, Sadeghpour, and Dalgarno (1998) into the X-ray absorption routine (VPHABS). Unlike the work discussed by Lieu *et al.* (1996a,b,c), we use the *ROSAT* data over the energy range 0.14-2.4 keV but we avoid the three softest channels, for which the calibration may be unreliable (Briel, Burkert, and Pfeffermann 1989; Snowden *et al.* 1995).

Successful single component fits were obtained for each of the objects (Table 3) for helium abundances of He/H=0.09 and 0.10. This range brackets most recent abundance determinations (Osterbrock, Tran, and Veilleux 1992; Baldwin *et al.* 1991), although Dupuis *et al.* (1994) find a somewhat lower value based upon *EUVE* observations of DA stars. Our model fits show a tight correlation between the He abundance and the column density: a reduction of 10% in He/H increases the derived column by $6.5 \pm 0.5\%$. As we discuss later, the effect is to bring the X-ray columns closer to their corresponding Galactic HI columns.

Spectral fits with He/H=0.10 are shown with their residuals in Figure 2. In region 1 of A1656 and A1795 and region 2 of A2199 the residuals show a small systematic modulation near 0.25 keV. This is due to a small error in the *ROSAT* calibration matrices which results in a slight offset in the peak of the response function. Because the offset is in the negative direction, it does not change our conclusion: if it is not due to calibration errors, it implies a either soft X-ray *deficit*, or a somewhat greater absorption column. As discussed above, in the case of Virgo the temperature was an additional fit parameter in the spectral modelling, and so we show confidence contours in $N_{H,x}$ and T in Figure 3.

3. Discussion and Conclusions

The study of the Virgo cluster was the work that established the studies of soft excess emission in clusters and motivated further work so we begin our discussion here. Our analysis leads to differences between the X-ray absorption column and the 21 cm HI column that are no greater than 1.3σ and the residuals are symmetric about zero (Table 3; Figure 2). The difference between our result and that of Lieu *et al.* (1996b)

is due primarily to the lower cross section that we used and secondarily to a lower 21 cm column density derived by Hartmann and Burton (1997). The difference between the 21 cm HI column of Hartmann and Burton (1997) and of Lieu *et al.* (1996b) is within the uncertainties of the two different techniques used and is probably caused by small calibration differences, as previously discussed in Arabadjis and Bregman (1998). When we use the 21 cm columns and cross sections used by Lieu *et al.* (1996b) we find excess soft emission as well, which nearly disappears when the intervening column in the model is allowed to be fit. Figure 4a is a monotemperature fit to the Virgo data which uses the Lieu *et al.* (1996c) value $N_{H,x} = 1.8 \times 10^{20} \text{ cm}^{-2}$ and fits for the cluster temperature, abundance, and metallicity. There does indeed appear to be excess emission from 0.14–0.30 keV, and the reduced chi-squared value of the fit, χ_r^2 , is an unacceptable 1.37. The Lieu study remedied this by introducing a second (lower) temperature component which lowered χ_r^2 to a marginally acceptable 1.3. Our fit (Figure 4b), which uses the Yan *et al.* (1998) He I cross section and allows $N_{H,x}$ to vary, eliminates the soft excess as well, with $\chi_r^2 = 1.12$. We note that the X-ray column densities that we obtained are similar to those obtained by Nulsen and Böhringer (1995), who used the absorption cross sections of Morrison and McCammon (1983), which are very similar to the Yan, Sadeghpour, and Dalgarno (1998) cross sections that we employed (see Figure 1). In summary, our X-ray absorption column densities, which are similar to some other studies, are not significantly different than the 21 cm HI column density, leading us to conclude that a soft X-ray excess at energies below 0.3 keV is not a required feature of the X-ray spectrum of the Virgo cluster.

For the other four clusters, the X-ray absorption column is generally within 2.5σ of the 21 cm column when $\text{He}/\text{H} = 0.10$, and within 1.8σ of the 21 cm column for $\text{H}/\text{He} = 0.09$ (Table 3; Figure 5). In Abell 2199, the X-ray column exceeds the 21 cm column, while for the three other clusters, it is lower than the 21 cm column. However, in only one location is the X-ray absorption column more than 3σ different than the 21 cm column, position 2 in the Coma cluster when using the larger He/H value of 0.10 (a 3.6σ difference). We find this rather weak evidence for concluding that the X-ray absorption column is lower than the 21 cm column.

As discussed previously (Arabadjis and Bregman 1998), these findings imply that the ionized layer responsible for the pulsar dispersion measure must be very highly ionized (at least 50% of the He in the form of He III), since it cannot contribute significantly to the X-ray absorption column. However, the ionized column is consistent with that associated with a hot Galactic halo, which has been confirmed as a feature of the Galaxy by two independent groups (Pietz *et al.* 1998; Snowden *et al.* 1998).

Future work will be able to reduce the uncertainties for several of these measurements.

The upcoming X-ray telescope *AXAF* should have an excellent calibration and it will have greatly superior spectral resolution compared to *ROSAT*, so the accuracy of the fit and the resulting determination of the X-ray absorbing column should be more accurate. Also, more accurate 21 cm measurements of the HI column will be possible with the Green Bank Telescope, which should become operational within the next year. However, a major source of uncertainty is the He/H ratio in the ISM, and unless future observations can help to decide how to handle dust corrections to photoionization with improved accuracy, this uncertainty will persist.

The authors would like to thank J. Irwin, M. Sulkannen, S. Snowden, F. Lockman, D. Hartmann, and C. Sarazin for their comments and suggestions that assisted us in this investigation. We would like to acknowledge financial support from NASA grant NAG5-3247.

REFERENCES

Arabadjis, J.S., and Bregman, J.N. 1998, *Ap. J.*, in press.

Arnaud, K.A. 1996, *Astron. Soc. Pac. Conf. Ser.*, 101, 17.

Baldwin, J.A., Ferland, G.J., Martin, P.G., Corbin, M.R., Cota, S.A., Peterson, B.M., and Slettebak, A. 1991, *Ap. J.*, 374, 580.

Bałucińska-Church, M., and McCammon, D. 1992, *Ap. J.*, 400, 699.

Bizeau, J.M., and Wuilleumier, F.J. 1995, *J. Electron Spectr. Rel. Phenom.*, 71, 205.

Briel, U.G., Burkert, W., and Pfeffermann, E. 1989, *X-ray Calibration of the ROSAT Position-sensitive Proportional Counter: the Energy Calibration*, in *EUV, X-Ray, and Gamma-Ray Instrumentation for Astronomy and Atomic Physics*, Charles J. Hailey and Oswald H. Siegmund, Eds., *Proc. SPIE*, **1159**, 263.

D'Acri, F., De Grandi, S., and Molendi, S. 1998, in *Active X-ray Sky: Results from BeppoSAX and Rossi-XTE*, in press; also astro-ph/9802070.

Dixon, W.V.D., Hurwitz, M., & Ferguson, H.C. 1996, *Ap. J.*, 469, L77.

Donnelly, R.H., Markevitch, M., Forman, W., Jones, C., David, L.P., Churazov, E., and Gilfanov, M. 1998, *Ap. J.*, 500, 138.

Dupuis, J., Vennes, S., Bowyer, S., Pradhan, A.K., and Thejll, P. 1994, *Bull. Amer. Ast. Soc.*, 184, 29.01.

Fabian, A. C. 1996, *Science*, 271, 1244.

Fabian, A.C., Nulsen, P.E.J., and Canizares, C.R. 1984, *Nature*, 310, 733.

Haisch, B., Bowyer, S., and Malina, R.F. 1993, *Journal of the British Interplanetary Society*, 46, 539.

Hartmann, D., and Burton, W.B. 1997, *Atlas of Galactic Neutral Hyrdogen*, Cambridge University Press.

Henke, B.L., Lee, P., Tanaka, T.J., Shimabukuro, R.L., and Fujikawa, B.K. 1982, *Atomic Data and Nuclear Data Tables*, **27**, 1.

Hwang, U., Mushotzky, R.F., Loewenstein, M., Markert, T.H., Fukazawa, Y., and Matsumoto, H. 1997, *Ap. J.*, 476, 560.

Lieu, R., Mittaz, J.P.D., Bowyer, S., Breen, J.O., Lockman, F.J., Murphy, E.M., and Hwang, C.-Y., 1996a, *Science*, 274, 1335.

Lieu, R., Mittaz, J.P.D., Bowyer, S., Lockman, F.J., Hwang, C.-Y., and Schmitt, J.H.M.M. 1996b, *Ap. J.*, 458, L5.

Lieu, R., Mittaz, J.P.D., Bowyer, S., Lockman, F.J., Hwang, C.-Y., and Schmitt, J.H.M.M. 1996c, *MPE Report*, 263, 557.

Marr, G.V., and West, J.B. 1976, *Atomic and Nuclear Data Tables*, **18**, 497.

Mittaz, J.P.D., Lieu, R., and Lockman, F.J. 1998 *Ap. J.*, 498, L17.

Morrison, R., and McCammon,D. 1983, *Ap. J.*, 270, 119.

Nulsen, P.E.J., and Böringer, H. 1995, *M. N. R. A. S.*, 274, 1093.

Osterbrock, D.E., Tran, H.D., and Veilleux, S. 1992, *Ap. J.*, 389, 305.

Pietz, J., Kerp, J., Kalberla, P.M.W., Burton, W.B., Hartmann, D., and Mebold, U. 1998, *Astron. Astrophys.*, 332, 55.

Samson, J.A.R., He, Z.X., Yin, L., and Haddad, G.N. 1994, *J. Phys. B*, 27, 887.

Sarazin, C.L., and Lieu, R. 1998, *Ap. J.*, 494, L177.

Snowden, S.L., Egger, R., Finkbeiner, D.P., Freyberg, M.J., and Plucinsky, P.P. 1998, *Ap. J.*, 493, 715.

Snowden S.L., Turner T.J., George J.M., and Yusaf R. 1995, OGIP Calibration Memo CAL/ROS/95-003.

White, D.A., Jones, C., and Forman, W. 1997, *M. N. R. A. S.*, 292, 419.

White, R.E. III, Day, C.S.R., Hatsukade, I., and Hughes, J.P. 1994, *Ap. J.*, 433, 583.

Yan, M., Sadeghpour, H.R., and Dalgarno, A. 1998, *Ap. J.*, 496, 1044.

Taylor, J.H., and Cordes, J.M. 1993, *Ap. J.*, 411, 674.

Table 1. The five clusters in the sample.

cluster	l^{II}	b^{II}	T, keV ^a	z ^a
A1367	234.80	+73.03	3.5	0.0214
A1656	58.16	+88.01	8.0	0.0231
A1795	33.81	+77.18	5.1	0.0621
A2199	62.93	+43.69	4.7	0.0299
Virgo	283.78	+74.49	1.6,1.7	0.0037

^aThe temperature T and redshift z are taken from White, Jones and Forman (1997) and references therein, except for Virgo, whose temperature in the two source regions are determined from a χ^2 fit.

Table 2. Observation and data analysis parameters.

cluster	$t_{\text{int}}^{\text{a}}$, ks	annulus ^b (1), '	photons (1)	annulus ^b (2), '	photons (2)
A1367	18.1	2-8	8777	8-14	12070
A1656	20.4	0-3 ^c	7508	0-3 ^c	4739
A1795	35.1	3-6	42567	6-9	25613
A2199	41.1	11-12	11190	0-3 ^d	11673
Virgo	10.1	9-12	33775	12-15	31659

^a t_{int} is the integration time for the observation.

^bTwo concentric source annuli (or disks in the case of Abell 1656) were constructed for each cluster, delineated by the inner and outer radius.

^cThe source regions in Abell 1656 consist of two circular regions near the emission center with radii of 3'. These were chosen in order to avoid galaxies near the cluster center.

^dIn order to avoid bright point sources the second source region in Abell 2199 is a circular region near the emission center with a radius of 3'.

Table 3. Column densities toward each cluster in the sample (in units of 10^{20} cm $^{-2}$).

cluster	He/H	$N_{H,x}(1)^a$	$N_{H,x}(2)^a$	$N_{H,21\text{cm}}^b$	N_e^c	$\frac{\Delta N}{\sigma}(1)^d$	$\frac{\Delta N}{\sigma}(2)^d$
A1367	0.10	1.87 \pm 0.16	1.65 \pm 0.19	2.20 \pm 0.110	0.531	-1.70	-2.51
	0.09	2.00 \pm 0.17	1.77 \pm 0.21			-0.99	-1.81
A1656	0.10	0.781 \pm 0.050	0.597 \pm 0.071	0.90 \pm 0.045	0.509	-1.77	-3.61
	0.09	0.836 \pm 0.053	0.639 \pm 0.076			-0.92	-2.96
A1795	0.10	0.909 \pm 0.026	0.909 \pm 0.017	1.04 \pm 0.052	0.525	-2.25	-2.40
	0.09	0.964 \pm 0.028	0.963 \pm 0.019			-1.29	-1.33
A2199	0.10	0.830 \pm 0.035	0.877 \pm 0.047	0.81 \pm 0.041	0.744	+0.37	+1.07
	0.09	0.889 \pm 0.037	0.939 \pm 0.051			+1.43	+1.97
Virgo	0.10	1.73 \pm 0.055	1.59 \pm 0.079	1.72 \pm 0.086	0.531	+0.10	-1.11
	0.09	1.86 \pm 0.060	1.71 \pm 0.085			+1.34	-0.08

^a $N_{H,x}$ and 1σ errors toward two different source regions in each cluster.

^b $N_{H,21\text{cm}}$ from Hartmann and Burton (1997).

^c N_e calculated using the model of Taylor and Cordes (1993).

^d $\Delta N/\sigma = (N_{H,x} - N_{H,21\text{cm}})/(\sigma_{\text{Xray}}^2 + \sigma_{21\text{cm}}^2)^{1/2}$.

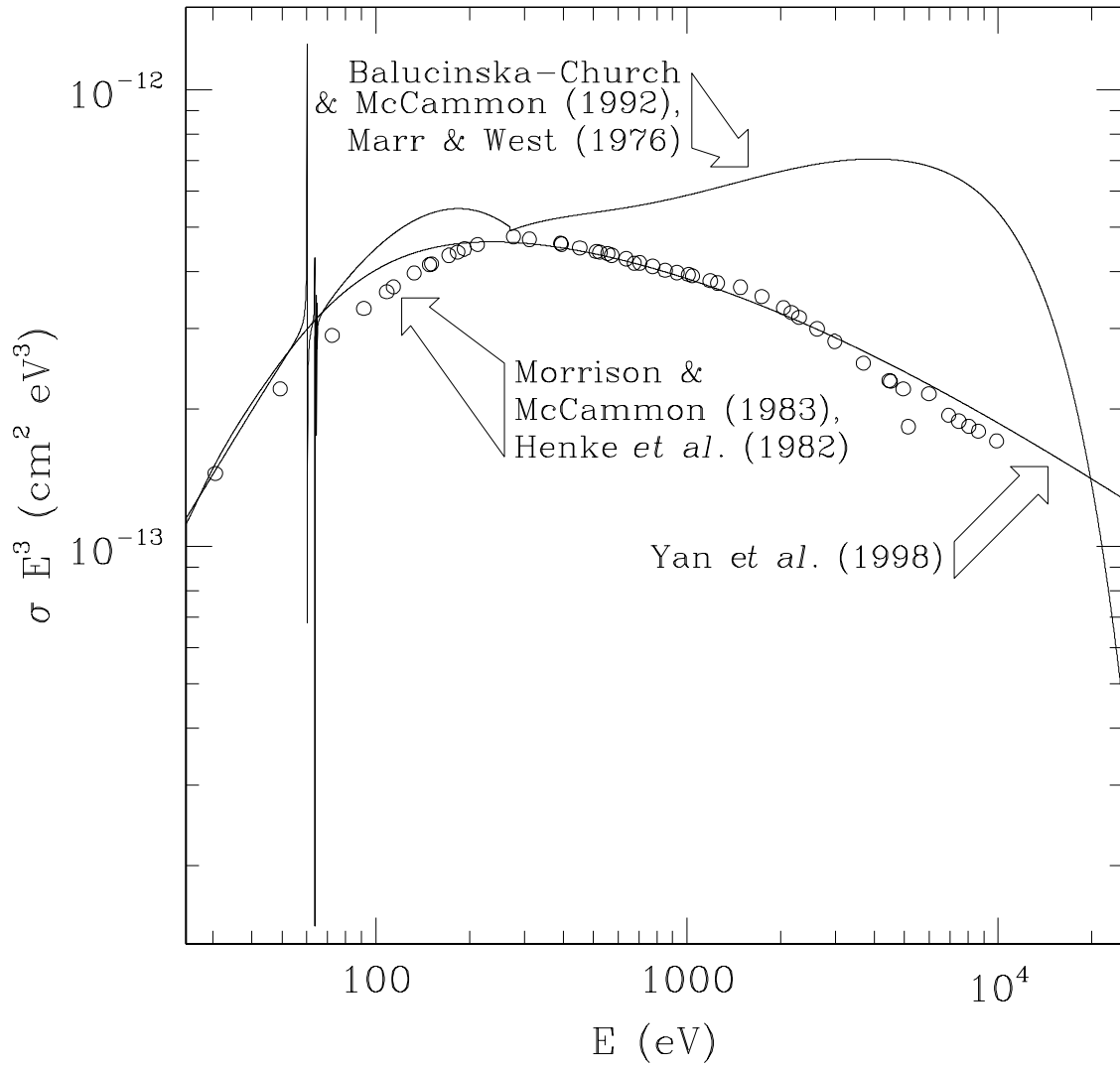
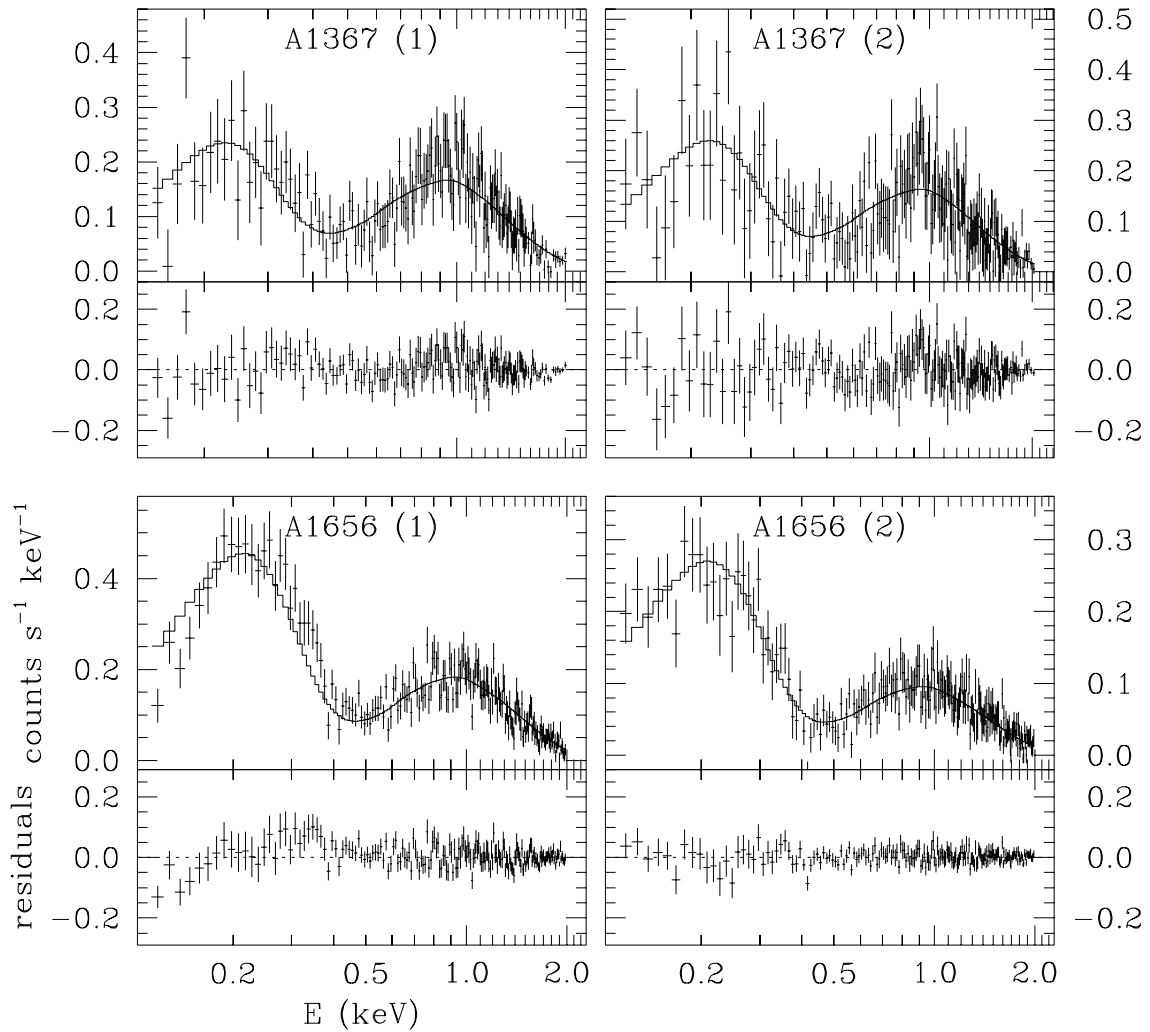
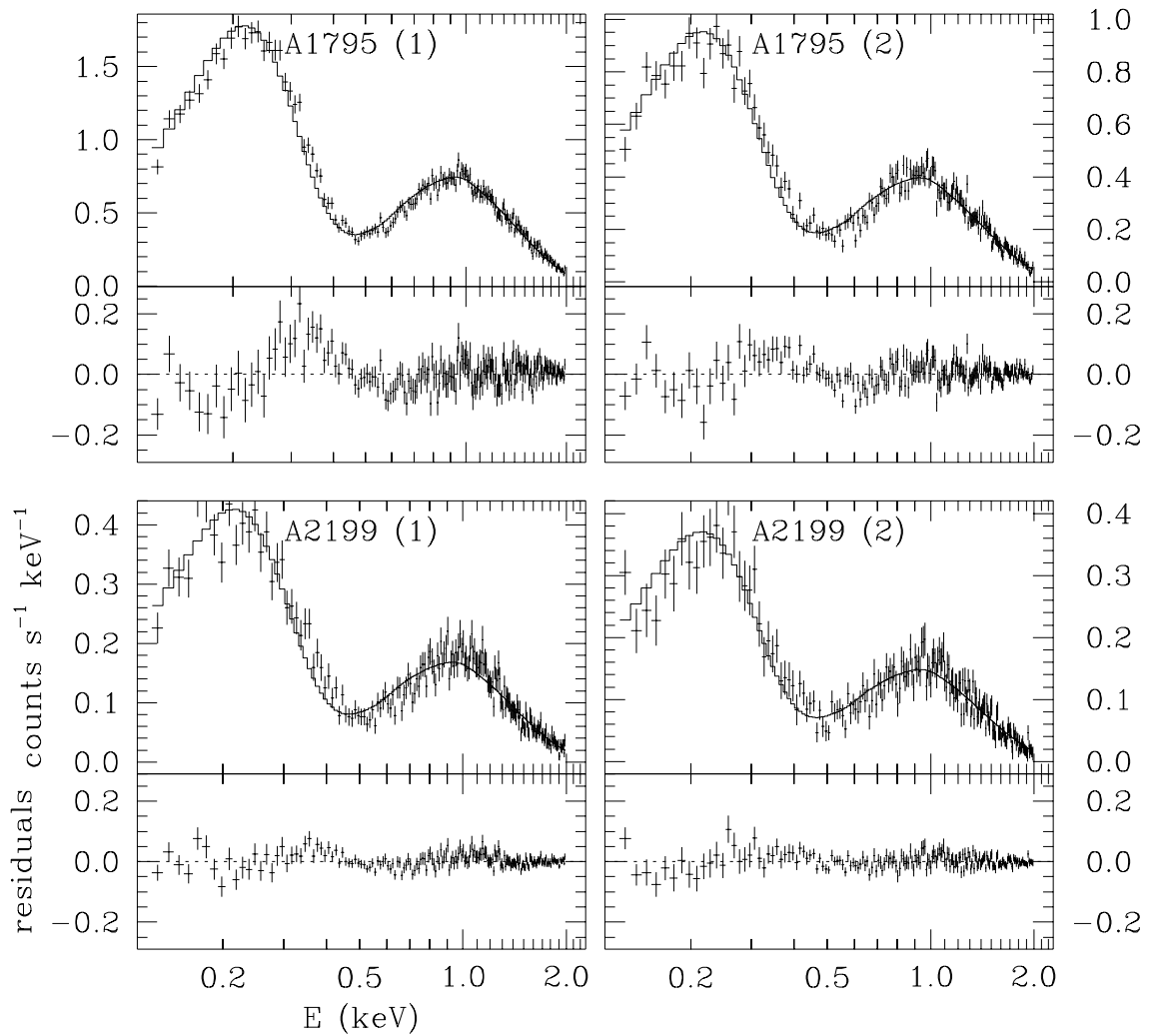


Fig. 1.— A comparison of neutral helium cross sections. The autoionization features near $E \sim 60$ eV are shown only for the Bałucińska-Church and McCammon (1992) cross sections. These are not relevant to our models, however, since the fitting range of this study is 0.14-2.0 keV.





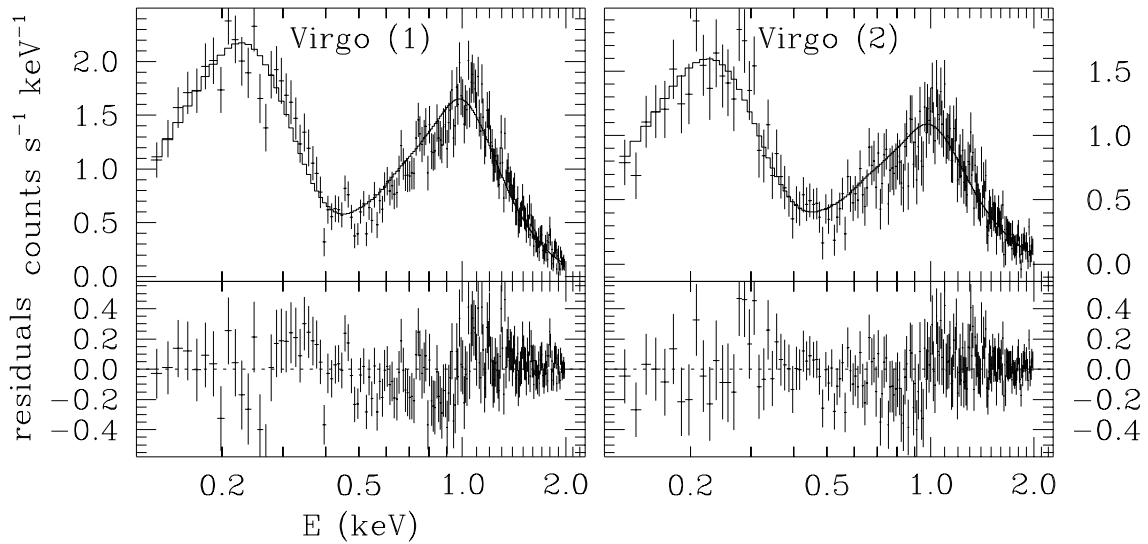
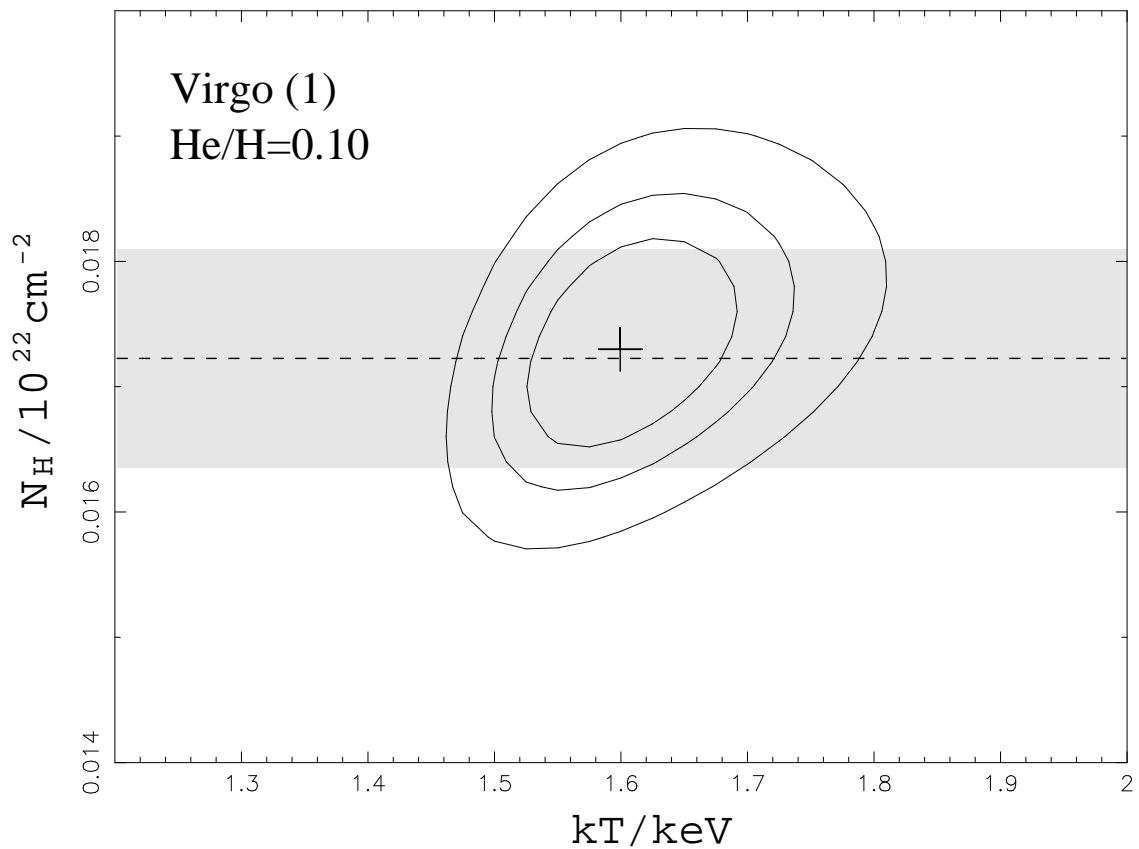
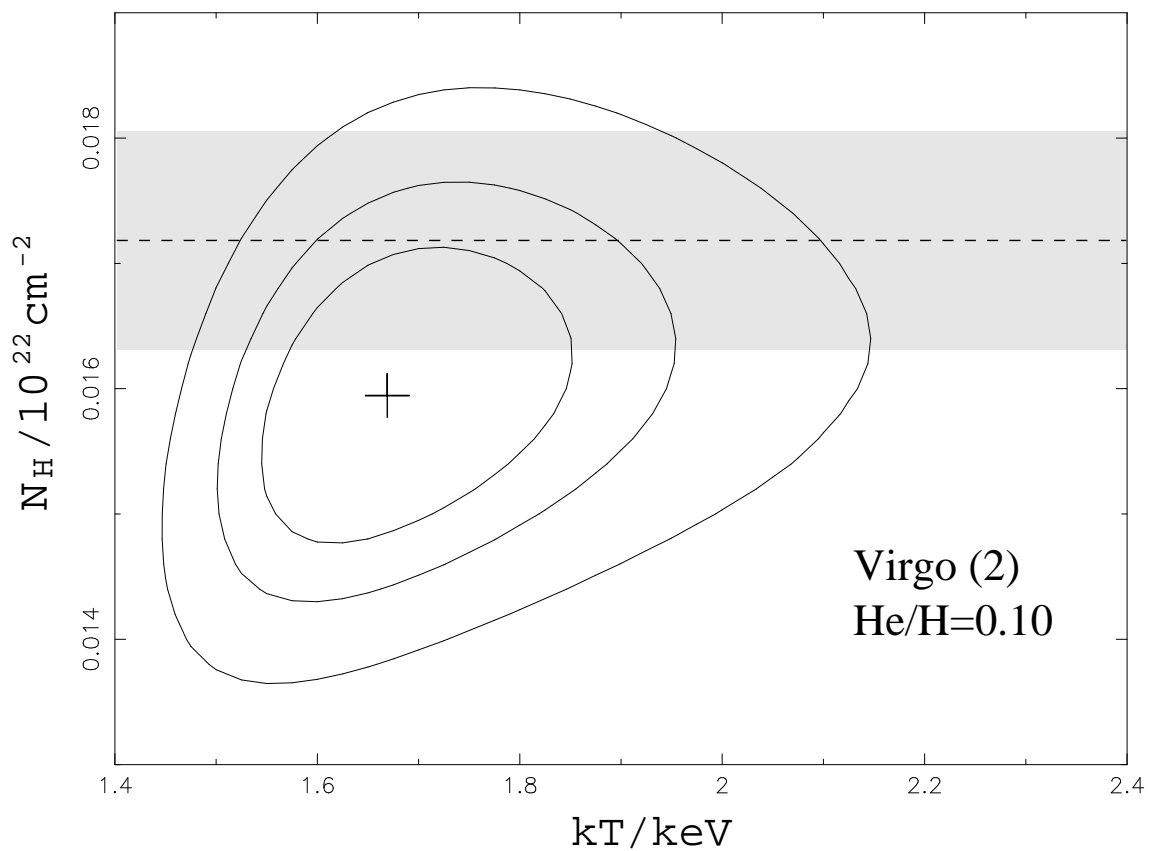
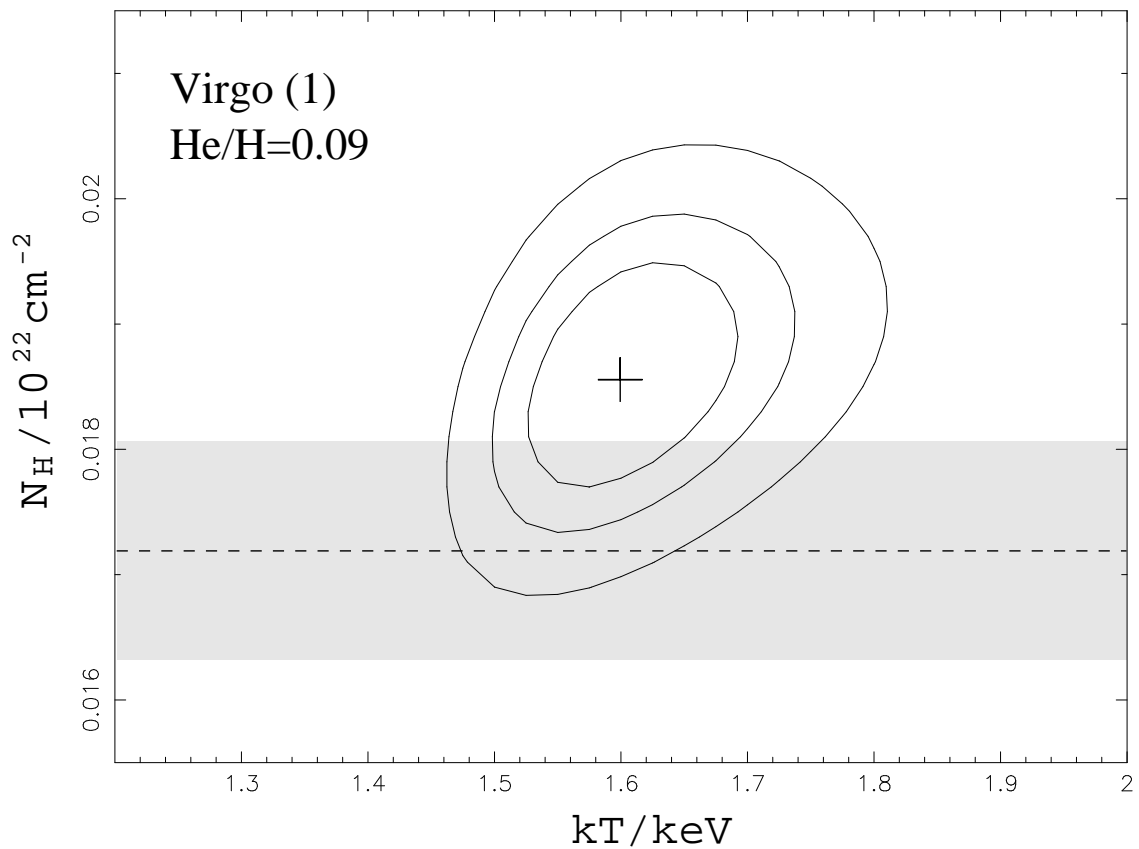


Fig. 2.— Spectral fits and residuals for the five clusters for a helium abundance of $\text{He}/\text{H}=0.10$.







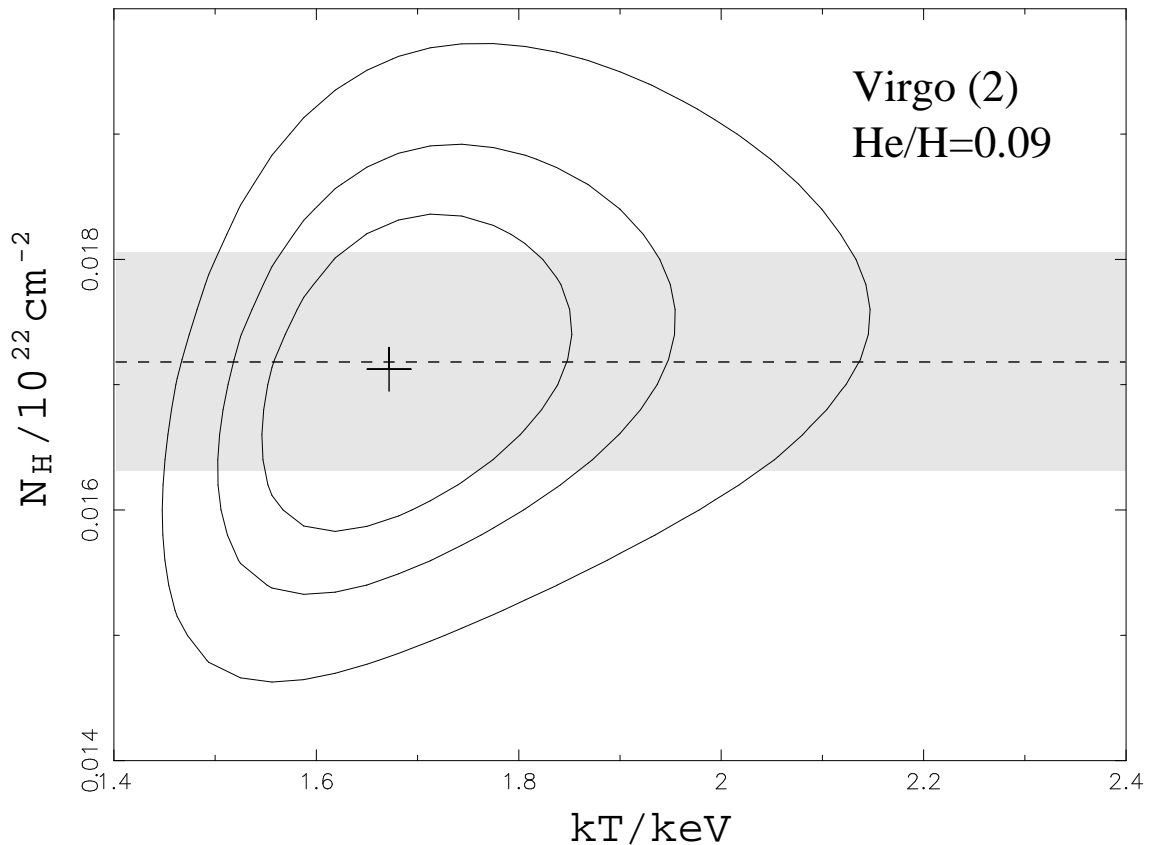


Fig. 3.— $\Delta\chi^2$ contours in parameters T and $N_{\text{H},x}$ for the Virgo spectral fits. Moving outward, the contours have values of 2.3, 4.6, and 9.2, corresponding to confidence limits of 68%, 90%, and 99%. The crosses indicate T and $N_{\text{H},x}$ of best-fit model. The 21 cm column and uncertainty (Hartmann and Burton 1997) is shown by the dashed lines and shaded regions, respectively.

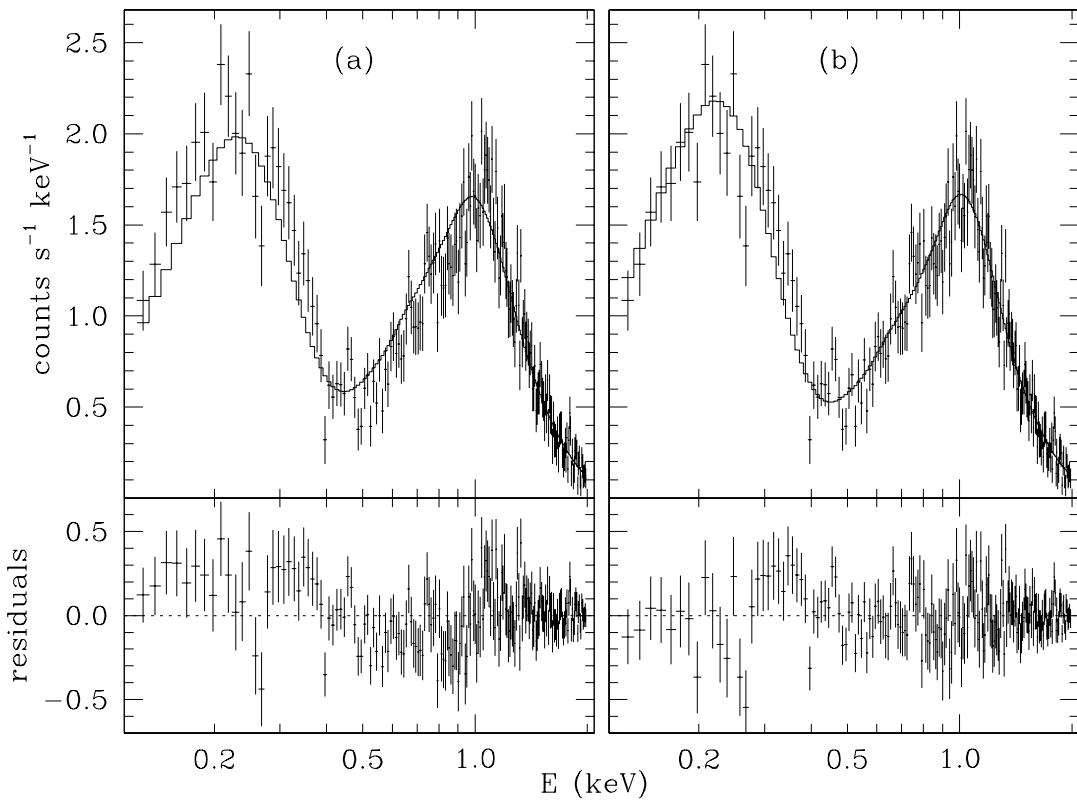


Fig. 4.— A monotemperature fit to Virgo using (a) $N_{\text{H},x} = 1.8 \times 10^{20}$ and the Bałucińska-Church and McCammon (1992) He cross sections, and (b) a variable $N_{\text{H},x}$ and and the Yan, Sadegpour, and Dalgarno (1998) He cross sections. Note the excess emission on 0.14-0.30 keV in (a) which is absent in (b).

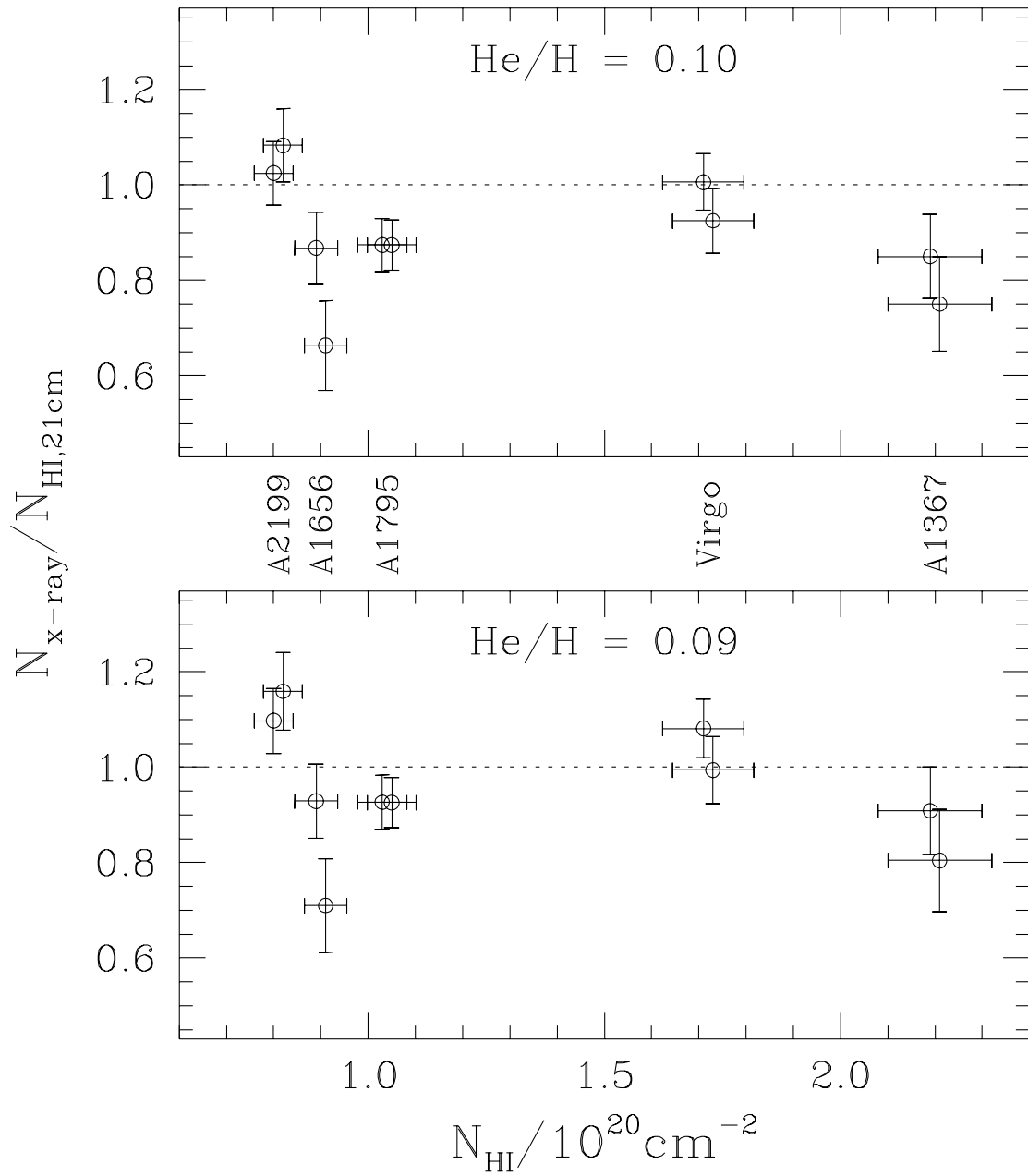


Fig. 5.— $N_{\text{H,x}}$ toward the five clusters for two different values of the assumed helium abundance.